Research Article | Vol. 25, No. 23 | 13 Nov 2017 | OPTICS EXPRESS 29013
Optics EXPRESS

Mode discrimination criterion for effective differential amplification in Yb-doped fiber design for high power operation

C. Molardi,[1,2] F. Poli,[1] L. Rosa,[3,4] S. Selleri,[1] and A. Cucinotta[1,*]

[1]*Department of Engineering and Architecture, University of Parma, Parco Area delle Scienze 181/A, I-43124 Parma, Italy*
[2]*Electrical and Electronic Engineering Department, School of Engineering, Nazarbayev University, Astana 010000, Kazakhstan*
[3]*Nanotechnology Facility, Center for Micro-Photonics, Swinburne University of Technology, Victoria 3122, Australia*
[4]*Department of Engineering "Enzo Ferrari", University of Modena and Reggio Emilia, via Vivarelli 10, 41124 Modena, Italy*
[*]*annamaria.cucinotta@unipr.it*

Abstract: The mode discrimination criterion for single mode operation, usually considered in fiber amplifiers designed for high power operation, has been investigated and tested on three different fiber designs, a large pitch fiber and two symmetry free photonic crystal fibers. To have a significant collection of results, parameters like pump configuration, pump power, and amplifier length have been varied. The analysis has been carried out through the use of a custom numerical tool provided with efficient thermal and spatial amplification models. From the obtained results, it is possible to observe that the mode discrimination criterion is helpful but not strictly necessary to pledge an effective single mode operation through differential amplification. This fact extends the possibility for the study, as well as for the optimization, of different fiber designs. The use of advanced numerical analysis, which takes into consideration amplification along with thermally influenced modes guidance, becomes extremely useful for an effective fiber design.

© 2017 Optical Society of America

OCIS codes: (060.2310) Fiber optics; (060.2280) Fiber design and fabrication; (060.5295) Photonic crystal fibers; (060.2320) Fiber optics amplifiers and oscillators

References and links

1. C. Jauregui, J. Limpert, and A. Tünnermann, "High-power fibre lasers," Nat. Photon. **7**(11), 861–867 (2013).
2. M. N. Zervas and C. A. Codemard, "High Power Fiber Lasers: A Review," IEEE J. Sel. Top. Quantum Electron. **20**(5), 219–241 (2014).
3. W. Shi, Q. Fang, X. Zhu, R. A. Norwood, and N. Peyghambarian, "Fiber lasers and their applications [invited]," Appl. Opt. **53**(28), 6554–6568 (2014).
4. P. Russell, "Photonic Crystal Fibers," Science **299**(5605), 358–362 (2003).
5. T. T. Alkeskjold, M. Laurila, J. Weirich, M. M. Johansen, C. B. Olausson, O. Lumholt, D. Noordegraaf, M. D. Maack, and C. Jakobsen, "Photonic crystal fiber amplifiers for high power ultrafast fiber lasers," Nanophotonics **2**(5-6), 369–381 (2013).
6. F. Stutzki, F. Jansen, H. Otto, C. Jauregui, J. Limpert, and A. Tünnermann, "Designing advanced very-large-mode-area fibers for power scaling of fiber-laser systems," Optica **1**(4), 233–242 (2014).
7. J. Limpert, F. Stutzki, F. Jansen, H. J. Otto, T. Eidam, C. Jauregui, and A. Tünnermann, "Yb-doped large-pitch fibers: effective single-mode operation based on higher-order mode delocalization," Light Sci. Appl. **1**, e8 (2012).
8. M. Laurila, M. Jørgensen, K. Hansen, T. Alkeskjold, J. Broeng, and J. Lægsgaard, "Distributed mode filtering rod fiber amplifier delivering 292W with improved mode stability," Opt. Express **20**(5), 5742–5753 (2012).
9. L. Dong, H. McKay, L. Fu, M. Ohta, A. Marcinkevicius, S. Suzuki, and M. Fermann, "Ytterbium-doped all glass leakage channel fibers with highly fluorine-doped silica pump cladding," Opt. Express **17**(11), 8962–8969 (2009).
10. X. Ma, C. Zhu, I. Hu, A. Kaplan, and A. Galvanauskas, "Single-mode chirally-coupled-core fibers with larger than 50μm diameter cores," Opt. Express **22**(8) , 9206–9219 (2014).
11. K. Saitoh and M. Koshiba, "Numerical modeling of photonic crystal fibers," J. Lightw. Technol. **23**(11), 3580–3590 (2005).

#298340 https://doi.org/10.1364/OE.25.029013
Journal © 2017 Received 19 Jun 2017; revised 3 Oct 2017; accepted 16 Oct 2017; published 8 Nov 2017

Optics EXPRESS

12. D. K. Sharma and A. Sharma, "Characteristic of microstructured optical fibers: an analytical approach," Opt. Quantum Electron. **44**(8), 415–424 (2012).
13. M. M. Jørgensen, S. R. Petersen, M. Laurila, J. Lægsgaard, and T. T. Alkeskjold, "Optimizing single mode robustness of the distributed modal filtering rod fiber amplifier," Opt. Express **20**(7), 7263–7273 (2012).
14. R. Dauliat, D. Gaponov, A. Benoit, F. Salin, K. Schuster, R. Jamier, and P. Roy, "Inner cladding microstructuration based on symmetry reduction for improvement of singlemode robustness in VLMA fiber," Opt. Express **21**(16), 18927–18936 (2013).
15. E. Coscelli, C. Molardi, M. Masruri, A. Cucinotta, and S. Selleri, "Thermally resilient Tm-doped large mode area photonic crystal fiber with symmetry-free cladding," Opt. Express **22**(8), 9707-9714 (2014).
16. E. Coscelli, C. Molardi, A. Cucinotta, and S. Selleri,"Symmetry-Free Tm-Doped Photonic Crystal Fiber With Enhanced Mode Area," IEEE J. Sel. Top. Quantum Electron. **20**(5), 544–550 (2014).
17. C. Molardi, B. Sun, X. Yu, A. Cucinotta, and S. Selleri, "Polarization-Maintaining Large Mode Area Fiber Design for 2-μm Operation," IEEE Photon. Technol. Lett. **28**(22), 2483–2486 (2016).
18. L. Wang, D. He, C. Yu, S. Feng, L. Hu, and D. Chen, "Very Large-Mode-Area, Symmetry-Reduced, Neodymium-Doped Silicate Glass All-Solid Large-Pitch Fiber," IEEE J. Sel. Top. Quantum Electron. **22**(2), 108–112 (2016).
19. F. Poli, E. Coscelli, A. Cucinotta, S. Selleri and F. Salin, "Single-Mode Propagation in Yb-Doped Large Mode Area Fibers With Reduced Cladding Symmetry," IEEE Photon. Technol. Lett. **26**(24), 2454–2457 (2014).
20. L. Rosa, E. Coscelli, F. Poli, A. Cucinotta, and S. Selleri,"Thermal modeling of gain competition in Yb-doped large-mode-area photonic-crystal fiber amplifier," Opt. Express **23**(14), 18638–18644 (2015).
21. F. Stutzki, F. Jansen, C. Jauregui, J. Limpert, and A. Tünnermann, "Non-hexagonal Large-Pitch Fibers for enhanced mode discrimination," Opt. Express **19**(13), 12081–12086 (2011).
22. D. C. Brown and H. J. Hoffman, "Thermal, stress, and thermo-optic effects in high average power double-clad silica fiber lasers," IEEE J. Quantum Electron. **37**(2), 207–217 (2001).
23. S. Hädrich, T. Schreiber, T. Pertsch, J. Limpert, T. Peschel, R. Eberhardt, and A. Tünnermann, "Thermo-optical behavior of rare-earth-doped low-NA fibers in high power operation," Opt. Express **14**(13), 6091–6097 (2006).
24. E. Coscelli, F. Poli, T. Alkeskjold, M. Jørgensen, L. Leick, J. Broeng, A. Cucinotta, and S. Selleri, "Thermal Effects on the Single-Mode Regime of Distributed Modal Filtering Rod Fiber," J. Lightw. Technol. **30**(22) , 3494–3499 (2012).

1. Introduction

Without any doubt, fiber laser research and technology have experienced great improvements in the last decade. Rare-earth doped fiber lasers offer clear advantages with respect to their counterparts based on active materials like semiconductors, crystals or gases. These advantages can be justified by several reasons, such as: the efficient heat dissipation of the fiber medium; the superior emission quality, thanks to the possibility to finely control the modal content of the amplified signal; and the capability to obtain a remarkable output power in the continuous wave regime or high energy short pulses in the pulsed one [1, 2]. For these reasons, rare-earth doped fiber lasers have found a wide spectrum of applications ranging from medical equipments to precise industrial micro-machining and to non-linear microscopy [3]. Actually, two important factors can be identified as the key of fiber lasers acceptance. The first is given by the use of Ytterbium as core dopant, mainly for the excellent energy conversion provided between pump and amplified signal. The second is the use of Double Cladding (DC) micro-structured fibers, which enhances pump absorption and permits to deliver higher power while preserving Single Mode (SM) operation and avoiding detrimental non-linear effects. Focusing on the latter key point, the introduction of Photonic Crystal Fibers (PCFs) and, more generally, of micro-structured fibers, has opened a new chapter in the field of photonics and fiber lasers technology [4]. The control over laser output modal content is no longer strictly bound to the engineering of refractive index contrast between the core and the cladding of the fiber, which actually presents some technological limitation. Instead, the mode content can be finely tailored with a proper design of the fiber cross-section geometry [5, 6]. This has impacted on the possibility to enlarge the core area, preserving the SM operation, with benefits on fiber laser and amplifier operation, in terms of output power. If, on one hand, this abundance of degrees of freedom has originated several fiber designs, such as: Large Pitch Fibers (LPFs), Distributed Mode Filtering fibers (DMFs), Leakage Channel Fibers (LCFs), and Chirally Coupled Core fibers (CCCs) [7–10], on the other hnad, fiber design has become much more complicated, requiring advanced numerical analysis tools [11, 12].

Optics EXPRESS

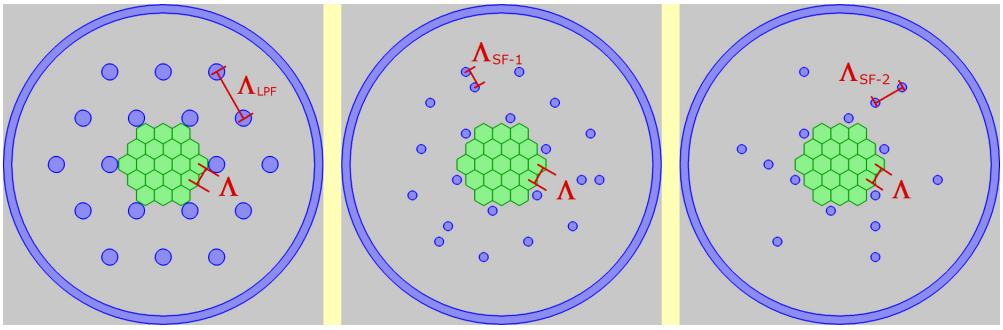

Fig. 1. Cross-section of: LPF (a); SF_1 (b); SF_2 (c).

In particular, several difficulties arise in evaluating the modal content and, consequently, in defining the proper parameters and their thresholds to obtain SM operation. This fact is much more evident in micro-structured fiber amplifiers for high power operation featuring a double cladding design, where the region of the pump cladding supports the coupling between cladding and core modes. To simplify fiber design directed to SM fiber amplifier operation, a criterion has been proposed in [13] and subsequently reused in [14–16]. This criterion is based on the evaluation of the mode overlap over the doped core area, defined as the normalized integral of mode intensity over the core area. It states that, in order to obtain an effective SM operation through the differential amplification mechanism, the Fundamental Mode (FM) overlap integral shall be higher than 0.8, while the overlap difference between FM and the most detrimental Higher Order Mode (HOM) shall be greater than 0.3. The application of this Mode Discrimination (MD) criterion, which has been originally proposed for Yb-doped rod-type DC PCFs [13], appears in some cases too restrictive and can be extended or improved, in particular when designs, not belonging to rod-type family, are explored [17, 18]. It is clear that a careful test of the MD criterion applicability range should be of benefit for fiber design.

In this contribution the MD criterion effectiveness has been deeply investigated by taking into consideration three different Yb-doped DC Large Mode Area (LMA) rod-type fiber designs. The fibers under exam are: a well-known LPF, a reference in the field of LMA design, and two asymmetric PCFs design, known as Symmetry Free (SF) PCFs, firstly proposed with all-solid design in [14], elaborated with holey cladding design for improving mode discrimination in Thulium doped fiber amplifiers [15, 16] and then investigated in the 1 μm region of operation, considering Ytterbium as the core dopant [19]. The amplification properties, as well as the modal content during gain competition have been investigated through the use of a custom-made spatial amplifier software, based on the Finite Elements Method (FEM) scheme, which implements the possibility of taking into account thermal effects on modes guidance during the amplification process [20]. With the help of this tool, the doped fibers performance has been studied considering different pump configurations, pump powers and doped fiber lengths.

This paper is organized as follows. The next section will describe the characteristics of the micro-structured doped fibers used in this analysis. In the third section the theoretical model and the numerical strategy used to test the MD criterion will be explained. In the fourth section results will be presented, comparing the fibers with co-propagating and with counter-propagating pump configuration. The last part of the section will be dedicated to investigate the MD criterion by varying the doped fiber length. Conclusions will be drawn in the final section.

Optics EXPRESS

2. Fiber designs under investigation

The cross-sections of the micro-structured Yb-doped fibers, considered in this analysis, are shown in Fig. 1. This three fiber designs share some common features. As it can be seen in the picture, the doped core is obtained by substituting the 19 innermost cells of the triangular lattice with Yb-doped rods. In order to have a fair comparison between these different designs, the distance between two neighboring cells, namely the pitch Λ, is set to 15 µm for all the fibers. Moreover the air cladding diameter, and consequently the inner cladding region size, is set to the same value of 17 times Λ. The air cladding thickness is 7 µm. As these are all rod-type doped fibers, outside the air cladding they present an outer cladding whose diameter is 1.7 mm. Another feature, common to the presented doped fibers, is related to the doping level which permits a pump absorption of 27 dB m^{-1}. While these parameters are common, all the considered designs differ in the strategy used to create the micro-structured inner cladding. In Fig. 1(a) a representative of LPF family, namely LPF45, is shown. The inner cladding is obtained by two rings of air holes organized in a periodic pattern. The distance between two neighboring holes, i.e. the pitch Λ_{LPF}, is set to a value of 45 µm. The diameter of each air hole is 13.5 µm. In Figs. 1(b) and 1(c), two fibers, which implement the idea of an asymmetric cladding design, are depicted. This is based on the fact that, removing the C_{6v} symmetry, the modes with circular shape, such as those belonging to the LP_{0x} family are poorly affected by the symmetry lost, while the modes with two-fold symmetry like the LP_{1x} ones show stronger delocalization. This designs aim is, consequently, the improvement of mode discrimination [14, 21]. As the inner cladding is no longer composed by a regular holes pattern, the pitch can be defined as the shortest distance between two neighboring holes. In agreement with this definition, the fiber SF_1, presented in Fig. 1(b), has a pitch $\Lambda_{SF\text{-}1}$ of 15 µm while the SF_2, shown in Fig. 1(c), has a pitch $\Lambda_{SF\text{-}2}$ of 26 µm. In both cases, the hole diameter is set to 7.5 µm.

3. Numerical analysis

The study has been performed through the use a custom-made numerical tool, which has been created by implementing a theoretical model that takes into account the propagation, the spatial mode gain along the doped fiber length, and the changes of guidance induced by thermal effects. The software logic follows some predefined operational steps [20]. At the beginning the modes of interest and their overlap integral with the fiber core, calculated through the use of a FEM modal solver, are supplied and used as input parameters. It is worth noting that the core overlap Γ of each mode is defined as the normalized field intensity $i(x, y)$, integrated over the doped core area, as show by the following formula:

$$\Gamma = \iint_{\text{core}} i(x, y)\, dx\, dy\,. \tag{1}$$

Subsequently, the input conditions of pump and signal power are set in order to start the propagation of the modes along the fiber, namely along the z direction. The fiber length is discretized in a number of small propagation steps. The pump absorption and the signal amplification are implemented solving for the coupled set of spatially defined population and propagation equations, i.e. considering the local interaction of the fields with the doped area.

During the propagation a thermal model is used to calculate the temperature distribution on the fiber cross-section. This model is implemented by assuming that the cross section is composed by a set of concentric regions characterized by different thermal conductivities. In this configuration, the heat source, induced by the quantum defect of pump-to-signal conversion, is located in the core region, which is approximated as a circle with the same area of the doped core. The external surface of the fiber is used to apply Newton's boundary condition, according to the implemented cooling system and the environment temperature [22, 23]. In the given case, an environment

Optics EXPRESS

temperature of 25 °C, and a forced-air convection coefficient h equal to 80 W m^{-2} K^{-1}, have been used. The other relevant parameters and coefficients, which are used in this model, can be retrieved from [24]. Despite the geometrical approximation, this model has shown to be accurate, with the additional advantage of being numerically efficient [24]. In agreement with the thermo-optical effect, the refractive index change is calculated starting from the temperature gradient induced by the heat density, by the help this thermo-optic relation:

$$\Delta n = \beta(T - T_0), \tag{2}$$

with the coefficient β equal to 1.16×10^{-5} K^{-1}, and T_0 the room temperature. The temperature gradient, calculated in the centre of the fibers under investigation, can reach the cap value of 160 K, at the output ending, in the case of backward pumping with a pump power of 400 W. Consequently, the induced refractive index gradient can touch the value of more than 2×10^{-3}. When the refractive index variation reaches a predefined small threshold, the software automatically updates the guidance properties by calculating again the field distribution and the core overlaps, in order to continue the propagation with the new values. This procedure is iterated step by step, forth and back along z, until the fields converge to a stable magnitude.

In this work, simulations have been performed by varying some parameters, which are supposed to be useful to test the SM overlap criterion. The pump has been set both in co-propagating and counter-propagating configuration, with a power varying from 25 W to 400 W. In all the simulations the pump wavelength is set to 976 nm. Regarding the input signal, its content has been considered composed by two modes, the FM and the first HOM. As the HOM confinement can be poor and several couplings between core and cladding modes can appear, the first HOM has been chosen as the most confined LP_{11}-*like* mode. The input power of these two input signals has been set to 5 W and 50 mW respectively. Such values represent a feasible modal content of a well-focused input [6]. The signal wavelength is set to 1032 nm. The influence of the length on the doped fiber amplifiers performance has also been investigated, by change its value from 60 cm to 120 cm.

4. Results and discussion

The amplification dynamics in rod-type doped fibers for high power operation amplifiers can be, most of the times, difficult to predict, as many factors play an important role in the output generation. The modal content is one of these factors, as it is directly related to the competition for gain resources. In principle a good mode discrimination at the beginning of the amplification process can bring to a lower HOM content at the ending of the doped fiber. Nevertheless this factor is to be evaluated in strict conjunction with the perturbation of the refractive index given by the heat density induced by the pump absorption. Since the heat density generated in the core tends to increase the refractive index of the core much more with respect to the cladding one, the result is of a stronger confinement of all the modes. This effect, known as thermal lensing, can transform a fiber which is SM at room temperature, to a multi-mode fiber under strong thermal stress [22]. It follows that the position, where the maximum absorption of pump is located, is influent on the final amplification behavior, and the pump configuration, co-propagating or counter-propagating, along with the length of the doped fiber can depict different scenarios at the output. Furthermore the fiber design, which can induce a higher mode discrimination as well as a stronger coupling between cladding and core modes, is determinant for the amplifiers performance. For the above-mentioned reasons, it has been chosen to evaluate three fiber designs with a different mode discrimination, taking into consideration different pump configuration and several pump power levels, with an overview on the doped fiber amplifier length.

Optics EXPRESS

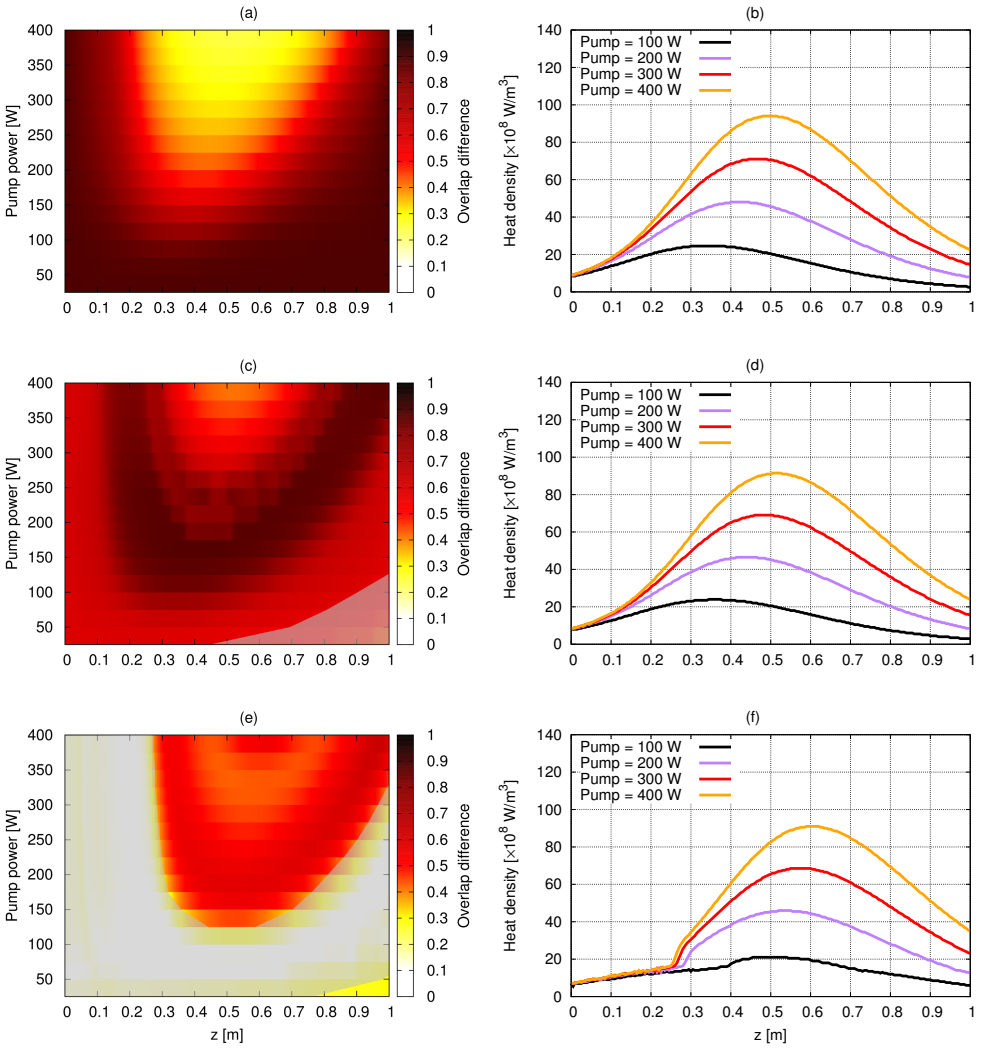

Fig. 2. Evolution on z of the overlap difference $\Delta\Gamma$ between the FM and the most detrimental HOM for : LPF (a); SF_1 (c); SF_2 (e). Evolution on z of the heat density for pump power values of 100, 200, 300, and 400 W, for: LPF (b); SF_1 (d); SF_2 (f).

4.1. Pump configuration, co-propagating case

For this pump configuration, a 1 m long doped fiber has been taken into consideration. From Figs. 2(a)-2(f), it is possible to appreciate the evolution, over the propagation direction z, of the overlap difference $\Delta\Gamma$ between the FM and the most detrimental HOM with LP_{11}-*like* shape, evaluated in the over-mentioned pump power range, as well as the heat density evolution over z for increasing values of pump power. The color maps, shown in Figs. 2(a), 2(c) and 2(e), depict three different guidance behaviors with respect to the design of the fibers under investigation, while the plots of Figs. 2(b), 2(d) and 2(f) depict the heat density of the corresponding fiber design. The chosen set of plots appears very useful to describe the fiber behaviour under thermal stress. The mapping of heat density gives information about the position and the intensity of maximum heat generated in the core, which has direct consequences on the refractive index variation and on

Optics EXPRESS

the induced thermal lensing effect. However this is not enough to have a complete picture of the situation, as different fiber designs can react to the index variation confining in different way the FM and the HOMs. The ability of a fiber to maintain a good HOMs delocalization is reflected on the overlap difference mapping. Since the dynamic of the overlap difference is not a simple function of the heat load, the use of an advance numerical model for amplification in presence of head load is absolutely necessary.

The LPF, as shown in Fig. 2(a), permits a very good mode discrimination both at the input and the output ending of the doped fiber, in the whole range of pump power. When the pump power increase over the value of 300 W, the middle part of the doped fiber shows a degradation of $\Delta\Gamma$ with a value smaller than 0.3. Looking at the heat density evolution, depicted in Fig. 2(b), this multi-mode behavior is induced by the maximum of heat density generation which appears at a distance of 50 cm from the input ending of the fiber. It is worth noting that the point of maximum heat moves toward the output ending with the increase of the pump power, this is because the spatial offset of maximum pump-to-signal conversion efficiency. Considering the SF_1, it is necessary to deliver some more comments. From Fig. 2(d) it is possible to see that the heat density generation is very similar to the LPF case, with a small difference on the maximum of the heat density, which is right shifted of 2 cm. With this heat density evolution, the SF_1 shows a better thermal resilience with respect the LPF. From Fig. 2(c) it is possible to see that the minimum of $\Delta\Gamma$ is larger than in LPF, with a value greater than 0.3. The price for having a better response to thermal effects is payed at the input end of the fiber where the mode discrimination is not so high as the one shown by the LPF. Regarding the efficiency of SF_1 to operate at different pump power values, it is possible to observe a good stability for the whole range of pump power, with the exception of the region under the 100 W where the FM overlap integral is decreasing under the value of 0.8. This occurrence is highlighted with the shaded region in Fig. 2(c). For high pump power the output mode discrimination $\Delta\Gamma$ returns to be very high, with peaks larger than 0.85. A different consideration shall be depicted for describing the behavior of SF_2. This fiber presents a more "open" cladding design, which permits larger coupling between the core and the cladding modes. In particular this fiber provides a poor FM confinement in condition of light heat load. From Fig. 2(e), it is possible to see the extension of the area, shaded in gray, where the FM overlap is less than 0.8. This area is also characterized by a mode discrimination $\Delta\Gamma$ which is quite lower than 0.3. The poor FM guidance region is induced by a low pump power, less than 150 W, or by a low pump-to-signal conversion, roughly found in the first 30 cm of amplification. Regarding to the latter consideration, it is possible to evaluate what is the mechanism which causes this behavior, by analyzing the the plot in Fig. 2(f). The poor confinement and the coupling of the FM with cladding modes, in cold fiber condition, do not permit an efficient pump conversion, so the heat density generation remains low in the first half of the doped fiber amplifier. Therefore, the amplification is spatially shifted until the thermal stress become intense enough to force a better FM confinement. The peak of maximum heat density generation is significantly shifted toward the output ending. However, after this phase, which can be defined as a warm-up, when strong pumping condition occurs, the mode discrimination becomes quite high and constant up to the output ending.

4.2. MD criterion discussion in co-propagating case

As the objective of this work is to discuss and test the MD criterion application range, it is firstly necessary to go deep into the MD criterion logic. The criterion states that, in order to obtain an enhancement of the FM over the first HOM, which represents the HOM suppression for gain competition, the FM core overlap shall be larger than 0.8, and the mode discrimination $\Delta\Gamma$, between the FM and the most confined HOM, shall be larger than 0.3. It is clear that these conditions should be verified in case of cold fiber. However, it also appears reasonable that such conditions can be extended in a larger operation region, for instance when the fiber is no

Optics EXPRESS

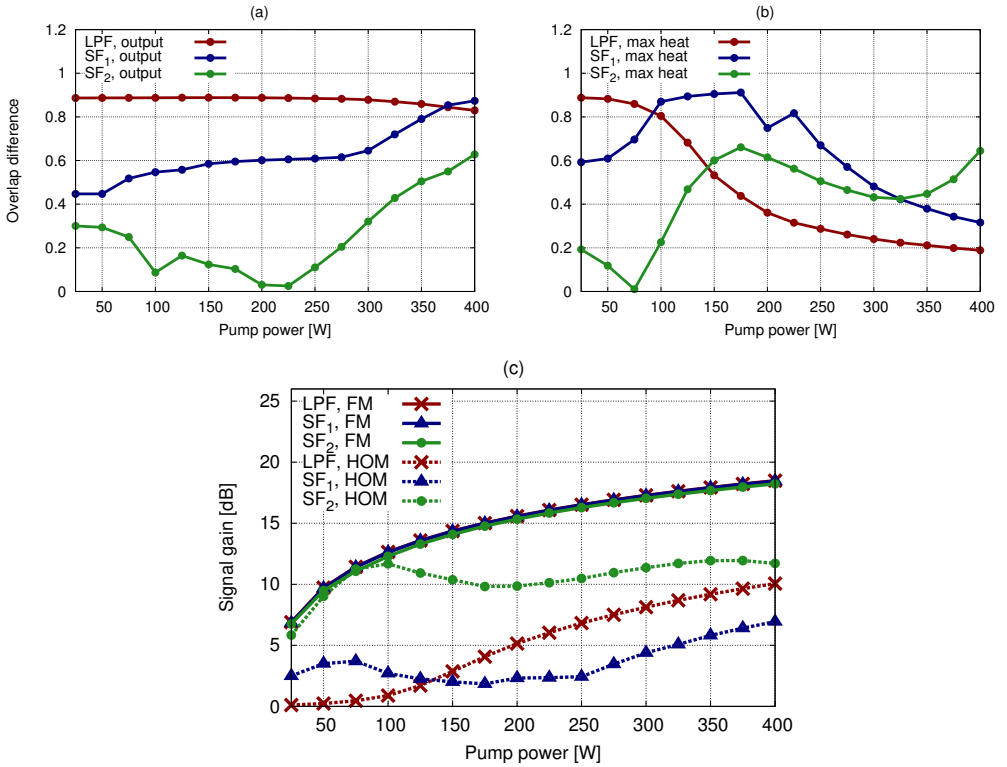

Fig. 3. Mode discrimination over the pump power: at the output ending (a); at the maximum of heat density (b). Gain of FM and HOM at the output ending after the process of amplification (c).

longer cold or at the end of the fiber, in order to prevent unwanted guidance artifacts during the amplification. Regarding the last consideration, as the output is composed by the superposition of two modes, following the prescription of MD criterion, not only the gain of the signal components is important in order to evaluate the output quality, but also the evolution of the relative modal content, namely the doped core overlap integral, is relevant. Therefore, the $\Delta\Gamma$ of the output and the $\Delta\Gamma$ of the position where the maximum of heat load is reached have been monitored over the considered pump power range. A similar treatment has been dedicated to the FM and to the HOM gain. The obtained data are shown in Fig. 3. Before to proceed, it is necessary to point out that the mode discrimination $\Delta\Gamma$ in "cold" condition is equal to 0.89, 0.41, and 0.28, respectively for the LPF, the SF_1, and the SF_2. Furthermore the SF_1 and the SF_2 FM overlap are less than 0.8. Consequently, while the MD criterion is fully enforced for the LPF, it is partially enforced for the SF_1 and not enforced at all for the SF_2. From Fig. 3(c) it is possible to see that the gain competition favours the FM with respect to the HOM in all the three cases, with a maximum increment of 8.42 dB, 11.50 dB, and 6.51 dB, respectively for the LPF, the SF_1, and the SF_2. In particular it is possible to notice that the best results are obtained by the SF_1 which partially fulfills the MD criterion. The LPF shows a better behavior at low pump power, while SF_2 appears not suitable for low power operation. It is also necessary to highlight that $\Delta\Gamma$ at the output, shown in Fig. 3(a), is also quite good for all the fiber under investigation at high pump power, with a larger range of operation shown by the LPF. On the other hand, from Fig. 3(b), it is possible to see that the best mode discrimination at the heaviest thermal stress is achieved by the SF_2.

Optics EXPRESS

These results demonstrate, by considering a co-propagating pump configuration, that the lack of the MD criterion recommendations, both partial or total, does not compromise the effectiveness of mode competition during the amplification process. As shown, in the case of SF_1, albeit the poor FM confinement in cold condition, the results depict a better differential amplification. Nevertheless, the total lack of MD criterion principles can result in a less efficient amplification, fostering a larger HOM content for fiber designs specialized to operate at higher thermal stress, as can be seen in the case of SF_2. Even though the MD criterion is always applicable and is useful in preliminary studies, its simple application, with no further investigations, can lead to exclude promising fiber designs. To better understand, case by case, whether a fiber design is effective or not for the amplification, the model which combines thermal effects and spatial amplification, used in this work, is necessary.

4.3. Pump configuration, counter-propagating case

As in the previous section, the same three fiber amplifier designs have been taken in consideration. Consequently their mode discrimination in "cold" fiber condition remains unchanged. The difference is given by the counter-propagating pump configuration. Results are shown in Figs. 4(a)-4(f). The overlap integral evolution along the positive propagation direction z is shown in Figs. 4(a), 4(c) and 4(e), respectively for LPF, SF_1, and SF_2. With respect to the same fiber designs, the heat density evolution along z is shown in Figs. 4(b), 4(d) and 4(f). Because of the counter-propagating pump, the peak of heat density generation is, in this case, concentrated at the doped fiber output ending, where the maximum of pump-to-signal conversion is located and where the signal to amplify is much more intense. A direct consequence of this fact is that the maximum of heat density assumes a value, around $170\,\mathrm{W\,m^{-3}}$, which is higher with respect to the co-propagating case, where it remains under $100\,\mathrm{W\,m^{-3}}$, for all the fibers under investigation, as shown in Figs. 4(b), 4(d) and 4(f). Another consideration is related to the heat density distribution along z direction, which is compressed on the last few centimeter of the fiber, forcing a faster degradation of the modes discrimination at the fiber output ending. In the case of LPF, as shown in Fig. 4(a), the mode discrimination $\Delta\Gamma$ remains very high with a constant value of 0.8, when the pump power is less than 50 W, gradually decreasing along z when pump increases. At a pump power of 400 W, the value of $\Delta\Gamma$ smaller than 0.3 is located in the range of z going from 62 cm to the end of the fiber, with a poor overlap discrimination at the output ending. Nevertheless the LPF shows a good mode discrimination and a superior FM guidance at the input ending in the whole considered power range. The SF_1 behavior is depicted in Fig. 4(c). While the evolution of heat density generation along z is actually similar to the LPF case, as it is possible to evaluate from Fig. 4(d), the doped fiber amplifier shows a better resilience to the heat generation in terms of mode discrimination, in particular at values of pump power larger than 200 W. At pump power of 400 W the z range where $\Delta\Gamma$ is less than 0.3 is restricted to the last 20 cm of the fiber. Even if this region is smaller with respect to the LPF, the mode discrimination decreases quite rapidly. The doped fiber shows a region of reduced FM guidance, with a core overlap smaller than 0.8, at the input ending the fiber, for values of input pump power lower than 200 W, as shown by the shaded region in Fig. 4(c). Analyzing the case of SF_2, similar considerations with respect the co-propagating configuration can be drawn. This fiber presents a poor FM confinement at the input ending, for all the range of considered pump power values, caused by the strong coupling between cladding and core modes. This fact impinges on the pump-to-signal conversion efficiency, which is reduced and shifted along the z direction, as it can be seen in Fig. 4(f), where the heat density generation shows a sudden change of slope. Consequently the region of high mode discrimination is reduced only to the regions of strong pumping operation. This affects the amplification efficiency. However the operation region, where the output $\Delta\Gamma$ is larger than 0.3, is extended in the pump power range between 60 W and 300 W, and, considering the pump power at 400 W, the output $\Delta\Gamma$ appears larger with respect to the other fiber amplifiers.

Optics EXPRESS

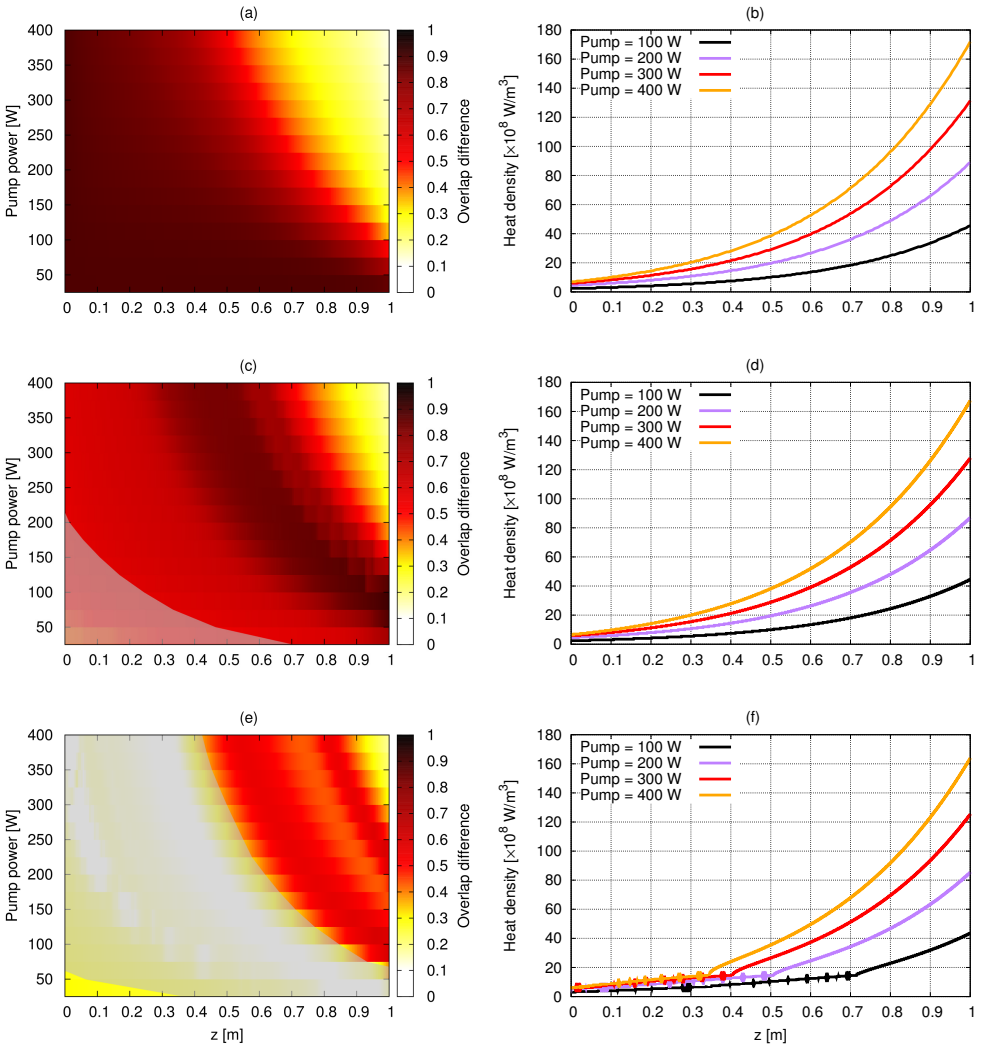

Fig. 4. Evolution on z of the overlap difference $\Delta\Gamma$ between the FM and the most detrimental HOM for : LPF (a); SF_1 (c); SF_2 (e). Evolution on z of the heat density for pump power values of 100, 200, 300, and 400 W, for: LPF (b); SF_1 (d); SF_2 (f).

4.4. MD criterion discussion in counter-propagating case

Regarding the gain competition and the amplification efficiency, the results are shown in Figs. 5(a) and 5(b). In the case of counter-propagating pump the maximum of heat density generation is always reached at the end of the fiber so $\Delta\Gamma$ at the output is equivalent to its maximum. This particular pump configuration induces a fast increment of heat density and, consequently, the reduction of mode discrimination is also quite sudden. So the three different cross-section designs show a similar behavior at high values of pump power, while the differences are restricted to the region of low and middle pump power operation. According to the curves of Fig. 5(a), where the output $\Delta\Gamma$ is plotted with respect to the increase of pump power, the doped fibers show a different operating response to the thermal stress. In particular the LPF results less effective to maintain a good mode discrimination at the output ending. The $\Delta\Gamma$ values at the output are, 0.11, 0.14,

Optics EXPRESS

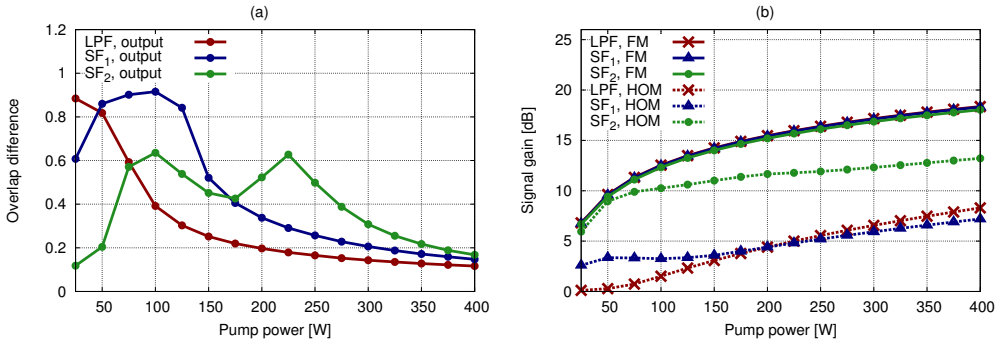

Fig. 5. Mode discrimination over the pump power at the output ending (a). Gain of FM and HOM at the output ending after the process of amplification (b).

and 0.17 respectively for the LPF, the SF_1, and the SF_2. Moreover, the region where $\Delta\Gamma$ is less than 0.3 is shifted toward lower pump power with respect to the co-propagating pump case, that is: 125 W for the LPF, 225 W for the SF_1 and 325 W for the SF_2. However, the behavior of the SF_2 in the low power region shows unwanted fluctuations. This clearly results in the degradation of the modal content of the output signal, as shown in Fig. 5(b). While the amplification of the FM is similar with respect to the different designs, with a slightly worse performance of 0.28 dB achieved by the SF_2, the HOM content varies significantly. In particular the SF_2 HOM content is 4.93 dB higher than the LPF, and 6.02 dB higher than the SF_2, when the pump power is 400 W. Consequently, the differential amplification is much more reduced for the SF_2, while it remains higher for the other designs. The values achieved are 10.06 dB, 11.10 dB, and 4.88 dB, respectively for the LPF, the SF_1, and the SF_2.

In summary, with regard to this pumping configuration, regardless the fibers are matching or not the recommendations of MD criterion, a certain amount of differential amplification for gain competition is achieved, with the worse observed performance in the case of SF_2, which is, indeed, the one which shows the larger discrepancy from the MD criterion recommendations. Furthermore, it is important to highlight that, because of the restriction of the effective amplifying region along z, and because of the higher heat generation in the output ending, the output mode discrimination is quite low for all the considered fiber designs, and in general poorer with respect to the co-propagating pump case. The best behavior, at high pump power, is achieved by the SF_1, which partially fits the MD criterion recommendations, while the LPF achieves the best results at low pump power. As stressed for the co-propagating case, the effectiveness of the presented fiber designs as well as their behavior can not be predicted or retrieved with the only use of MD criterion. Consequently, the use of a spatial amplifier simulator combined with thermal effects is enormously useful.

4.5. Doped fiber length dependency

In order to investigate the amplification performances with respect to the doped fiber amplifier length, the LPF has been chosen as a reference. This choice is driven by the LPF behavior, which appears stable over a large range of pump power, showing an evolution of the FM and the first HOM not affected by unwanted and detrimental mode coupling between core and cladding modes. This permits to draw simple considerations avoiding further discussions which could emerge by the occurrence of coupling issues. Moreover such considerations can be extended to the whole range of investigated pump powers. Consequently, the choice of a particular pump power value does not invalidate the analysis. For the next investigation, the LPF has been studied

Optics EXPRESS

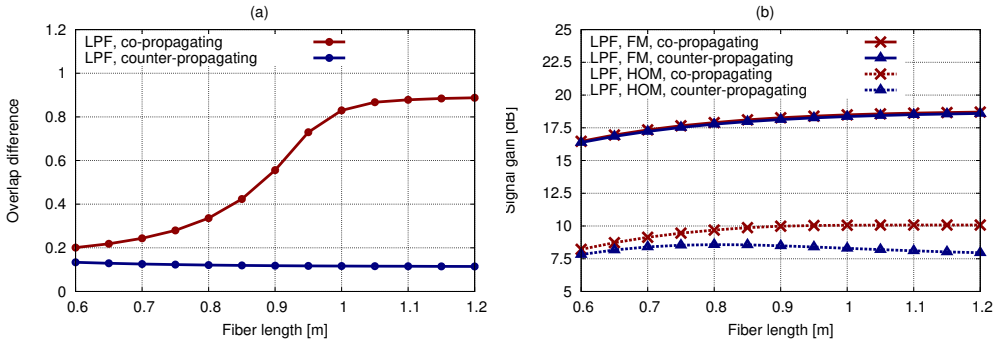

Fig. 6. Mode discrimination over the doped fiber length at the output ending (a). Gain of FM and HOM for different fiber lengths (b).

by considering a pump power of 400 W, both with co-propagating and counter-propagating configuration, varying the fiber length from 60 cm to 120 cm.

Considering that the fiber under investigation is perfectly in agreement with the MD criterion, the results, which are shown in Figs. 6(a) and 6(b), depict an interesting dependency from the doped fiber length, and from the pump configuration. As it is possible to see, one of the most evident differences between the two pump configuration is given by the mode discrimination at the amplifier output, which is poorly dependent on the fiber length for the counter-propagating pump, while it is strongly influenced by the same parameter for the co-propagating one. In particular, regarding the co-propagating configuration, for fibers shorter than 75 cm the mode discrimination, namely the overlap difference $\Delta\Gamma$, is less than 0.3, and increases for longer fibers. For the counter-propagating pump case, instead, the $\Delta\Gamma$ slightly decreases from 0.13 to 0.11. This behavior is strictly related to the position of maximum heat density generation, which is always at the output ending for the counter-propagating pump, while it can move from the output ending to a position in the middle of the fiber for the co-propagating pump. This can influence the effectiveness of the amplification and in particular the modal content at the fiber end. From Fig. 6(b), it is possible to appreciate the evolution of the FM and the first HOM gain for co-propagating and counter-propagating pump. The FM gain increases from 16.4 dB to 18.6 dB with a small offset of 0.1 dB with respect to the different pump configuration. The most evident difference is given by the evolution of the HOM content, which increases for the co-propagating pump setup, while it decreases for the counter-propagating one, as the length of the doped fiber increases. Considering a 120 cm long doped fiber, the differential amplification results in a differential gain of 10.63 dB for the counter-propagating case and of 8.61 dB for the co-propagating pump. Nevertheless, it is worth noting that the overlap integral of the first HOM, and consequently its distribution over the fiber cross-section is different, being confined in the core for the counter-propagating case, and spread in the cladding for the co-propagating pump.

As emerged from these observations, the fiber amplifier length influences the modal content of the output beam, making the process of gain competition less or more efficient with respect to the HOM suppression given by the differential amplification. Even considering the case of LPF, which shows an excellent behavior in terms of amplification properties, and it is full compliant in terms of MD criterion, the differential amplification can vary of some dB with the increase of the fiber length, in particular for the co-propagating pump configuration.

Optics EXPRESS

5. Conclusion

In this paper the range of validity of mode discrimination criterion for effective single mode operation induced by differential amplification has been investigated. Three rod-type Yb-doped PCF amplifiers, with different fiber cross-section designs and different responses to the thermal stress, have been taken in consideration. The analysis have been carried out with a FEM based numerical tools. In particular, the behavior of the doped fibers under investigation has been simulated through the use of a custom software provided with a spatial amplification model which takes in consideration the guidance changes induced by thermal effects. In order to obtain a wide spectrum of results to better test the MD criterion, different parameters have been selected and varied during the simulations. Among them, both co-propagating and counter-propagating pump configuration have been taken in consideration varying the pumping power from 25 W to 400 W. The fiber amplifier length has been also changed from 60 cm to 120 cm. The pump and the input signals wavelength has been set to 976 nm and 1032 nm, respectively. Furthermore the input signal has been considered composed by two components, the FM, characterized by an initial power of 5 W, and the first HOM with a power of 50 mW. From the results, obtained by the analysis of the selected doped fibers, it is possible to see that the application of MD criterion gives a strong margin of safety, in terms of fiber design, for obtaining an effective HOM suppression through differential amplification. However the application of all the MD criterion recommendations is not strictly necessary. In particular the reported examples show that an excellent single mode operation can be achieved when the MD criterion is partially satisfied, i.e. when $\Delta\Gamma$ is less than 0.3 but the FM core-overlap is not higher than 0.8. When MD criterion is totally disregarded the efficiency of the amplification is reduced but not compromised. In general, the fulfillment of MD criterion is shown to have an impact on the mode discrimination of the doped fiber output ending, inducing a change of output beam composition. In this context, the length of the doped fiber influences the mode discrimination at the output ending with different impact with respect to the pump configuration. The considerations, emerged form this analysis, create a larger margin for fiber design and amplification optimization. The MD criterion remains a valid help for a preliminary fiber design, however it has been demonstrated to be quite conservative. A more accurate and largely optimized designs can be addressed by a careful numerical analysis directed to the investigation of modal content during the amplification process, considering the thermal driven change of guidance properties. Under this point of view, the model used in this work has been demonstrated to be a necessary and powerful tool to achieve a better understanding of fibers behavior.

155.185.137.52 {ts '2020-02-13 04:38:46'}